Investigation of Ferroresonance in Offshore Wind Farms

Ebrahim A. Badran[*], Mohammad E. M. Rizk, and Mansour H. Abdel-Rahman

Electrical Engineering Department, Faculty of Engineering, Mansoura University, Mansoura, Egypt
[*]ebadran@mans.edu.eg

Abstract: Up to date, many literatures have investigated ferroresonance in electrical systems particularly distribution systems due to abnormal switching operations. Ferroresonance has bad effects on the insulation system and causes damages to surge arresters also. Recently, many researchers have investigated electromagnetic transients in offshore wind farms after the wide penetration of offshore wind farms in many countries as a renewable source of electricity. However, ferroresonance phenomenon has not been investigated in offshore wind farms. This paper investigates ferroresonance phenomenon and its bad effects in offshore wind farms. The PSCAD/EMTDC program is used for modeling the offshore wind farm. The offshore wind farm investigated in this study consists of 72 wind turbines arranged in eight rows. Ferroresonance in offshore wind farm in this investigation is produced by three different abnormal switching operations. The results show that the transient overvoltages produced by ferroresonance have bad effects on the insulation of both submarine single-core cables and the transformers. The results show also the surge arrester damage due to the continuity of ferroresonance phenomena. Furthermore, this paper suggests a protective method for suppression the ferroresonance in offshore wind farms. The results show that the proposed protective method against ferroresonance gives high suppression to ferroresonance in offshore wind farms.
[Ebrahim A. Badran, Mohammad E. M. Rizk, and Mansour H. Abdel-Rahman **Investigation of Ferroresonance in Offshore Wind Farms**. Journal of American Science 2011; 7(9):941-950]. (ISSN: 1545-1003). http://www.americanscience.org.

Key Words: Offshore Wind Farms, Ferroresonance Phenomenon, Abnormal Switching Operations, Wind Turbine Transformer (WTTs), Single Core Submarine Cables, Capacitor Banks.

1. Introduction

Recently, there has been a particular interest in the installation of collection grids of large offshore wind farms. The increasing penetration of offshore wind farms in many countries has brought problems involving electromagnetic transients to be an important subject. The electrical conditions present in the offshore wind farm collection grids are not alike any other electrical grids. The length of medium voltage (MV) submarine cables is remarkable; as well as the number of switchgears and transformers. This combination of components creates an electrical environment which is subjected to a lot of electromagnetic transient phenomena [1, 2].

In the literature, most researches have widely discussed electromagnetic transients such as overvoltages due to cable energizing and transformers inrush currents [1-4]. These electromagnetic transients are produced by normal switching operations in offshore wind farms. However, there are still some electromagnetic transients due to abnormal switching operations such as ferroresonance which are not investigated in offshore wind farms.

Ferroresonance is a complex nonlinear dynamic electrical phenomenon, which frequently occurs in a power system that comprises no-load saturated transformers, transmission lines (or cables) and single-phase switching with three-phase supply. Ferroresonance phenomenon causes dielectric and thermal problems in electrical systems [5-7]. Many researchers have investigated the ferroresonance phenomenon and its bad effects on the electrical systems particularly in distribution systems [6-10]. However, there are still a lot of work needed for the investigation of ferroresonance in offshore wind farms.

In this paper, ferroresonance phenomenon in offshore wind farm is investigated. The effect of ferroresonance on the surge arresters and on the insulation of both cables and transformers are demonstrated. A proposed protective method is presented for the suppression of the overvoltages that produced by ferroresonance. This protective method protects also the surge arresters against burnout due to the heat generated by ferroresonance.

The PSCAD/EMTDC program is used for modeling the offshore wind farm which consists of 72 wind turbines arranged in eight rows. Three abnormal switching operations which are responsible for occurrence of ferroresonance in the wind farm are investigated. The first switching operation is the blowout of the two fuses of phases B and C on the 33 kV side of WTT #A1 while the second one is the blowout of two fuses on the 33 kV side of WTT #A9. The third switching operation is the de-energization of phase C of a row A.

2. Description of the Investigated Offshore Wind Farm

Fig. 1 shows the single line diagram of the investigated offshore wind farm. It consists of 72 wind turbines arranged in array of 8 rows which are named from A to H. Each wind turbine is rated at 2.3 MW and 0.69 kV. Each turbine is connected to a WTT. The distance between each wind turbine and the adjacent one in each row is 505 m. Each row is separated from the adjacent one by a distance of 850 m [1, 2]. The WTTs of each row are connected to each other by 33 kV (MV) submarine cables. Each row is then connected to the platform by one root submarine cable. The distance between the platform and last wind turbine (*i.e.* WT #9) in the row is 7 km. The wind farm transformer is rated at 180 MVA and 132/33 kV. It is located in the central position and it has one high voltage winding and two MV windings. Each MV winding is connected to four rows as shown in Fig. 1.

The single-core submarine cables between the wind turbines are connected on the bottom of each wind turbine where the armor and the sheath of the cables are grounded. The WTT is rated at 2.5 MVA and 33/0.69 kV. It is connected to the submarine cables via a switch disconnecting fuse on the MV side.
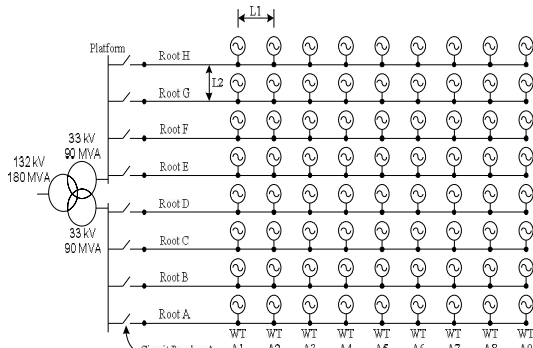

Fig. 1. The offshore wind farm configuration. (L1 = 505 m, L2 = 850 m)

A capacitor bank is included on the LV side of each WTT to compensate the drawn reactive power of the induction generators. Furthermore, included in the wind farm model is the connection of the wind farm transformer via a single three-phase high voltage (HV) sea cable (132 kV /10.5 km) and land cable (132 kV /18.3 km) to the grid connection point on land.

3. Modeling of the Electric Components of the Offshore Wind Farm using PSCAD/EMTDC

In this section, the detailed modeling of the electric components of the offshore wind farm using

the PSCAD/EMTDC is demonstrated. These components include submarine cables, transformers, power system grid, surge arresters, and capacitor banks.

A. System Modeling for Switching Study

In this subsection, the main guidelines for the modeling of the offshore wind farm for ferroresonance phenomenon investigation at row A are presented as:

1. The grid is modeled as an ideal voltage source.
2. Rows E, F, G, and H are modeled as one three-phase open ended single-core cables (root cables only) because they are connected in parallel.
3. Rows B, C, and D are modeled in the same way as rows E, F, G, and H.
4. Row A is modeled in details (from platform to WT #A9).

B. **Cable Parameters Calculation**

The MV single-core submarine cables are the most distinctive electric component in the offshore wind farms. The geometric configuration of the 33 kV three-phase single-core submarine cables between the WTTs is calculated based on the power transferred through them [11], and given in Table 1. In submarine cables, the armor is usually quite thick [12]. Therefore, it is assumed in this study that, an armor of 5 mm steel wires thickness. Also, an outer insulation of 5 mm thickness are incorporated into the three-phase single-core submarine cable design. So, the overall outer diameter of the cable is 65 mm. Fig. 2 shows the geometric configuration of the MV submarine cable.

The MV (33-kV) submarine cables, , are modeled using the frequency dependent (phase) model. This model represents the frequency dependence of internal transformation matrices [16]. The HV (132 kV) sea and land cables, are modeled using the PI equivalent sections to avoid the numerical errors due to the long length of the HV cables. The PI equivalent parameters are calculated from the cable geometric dimensions and its materials using Bergeron model at 50 Hz. Table 2 gives both positive and zero sequence resistance, inductive and capacitive reactance of the HV sea and land cables in the wind farm.

The cable core data entries for the PSCAD/EMTDC are manipulated as explained by[13]. The main insulation of high voltage cables is based on extruded insulation type and is always sandwiched between two semi-conductive layers. Unfortunately, the PSCAD/EMTDC does not allow the user to directly specify the semiconducting layers [14–15]. These must, therefore, be introduced by a modification of the input data by allowing the insulation to extend between the core conductor and

sheath conductor, and increasing the permittivity proportionally to leave the capacitance unaltered.

Table 1:   Geometric Dimensions of the 33-kV Single-Core Cable.

Cross section of conductor (A_c) [mm]^2	240.0
Diameter of conductor (d_2) [mm]	18.1
Insulation thickness (T_{ins}) [mm]	8.0
Diameter over insulation (Do_{ins}) [mm]	35.7
Cross section of screen (A_{sh}) [mm]^2	35.0
Outer diameter of cable (Do) [mm]	45.0

Table 2: 132 kV Single-Core Cables Data at 50 Hz.

The 132 kV land cable (equivalent PI section model)	
length	18300.0 [m]
+ve sequence resistance	0.0870615666 [m ohm/m]
+ve sequence inductive reactance	0.122644966 [m ohm/m]
+ve sequence capacitive reactance	9.091530621 [M ohm*m]
zero sequence resistance	0.186524753 [m ohm/m]
zero sequence inductive reactance	0.0551011310 [m ohm/m]
zero sequence capacitive reactance	9.091530621 [M ohm*m]
The 132 kV sea cable (equivalent PI section model)	
length	10500.0 [m]
+ve sequence resistance	0.0863663070 [m ohm/m]
+ve sequence inductive reactance	0.122711970 [m ohm/m]
+ve sequence capacitive reactance	9.091530621 [M ohm*m]
zero sequence resistance	0.182742143 [m ohm/m]
zero sequence inductive reactance	0.0619589991 [m ohm/m]
zero sequence capacitive reactance	9.091530621 [M ohm*m]

The semi-conductive layer thickness is computed as given by [13–15].   Both core and sheath of the submarine cable are made of copper.   The resistivity of the surrounding ground depends strongly on the soil characteristics.   The resistivity of sea water lies between 0.1 and 1.0 Ω.m [12]. The ground resistivity is assumed to be 1.0 Ω.m in this study.

C. Transformer Modeling

PSCAD/EMTDC offers two different transformer models when it comes to the saturation modeling. The first model is the classical modeling approach which does not take into account the magnetic coupling between different phases.   The second model is the unified magnetic equivalent circuit (UMEC) transformer models which are based primarily on core geometry.   For the transformer model based on the UMEC algorithm, phases are magnetically coupled [16].   The air core reactance

for the classical model approach is chosen as twice the positive sequence leakage reactance [17].

The WTTs are modeled using the UMEC model while the wind farm transformer is modeled using the classical approach model. Table 3 gives the data required for transformers modeling.
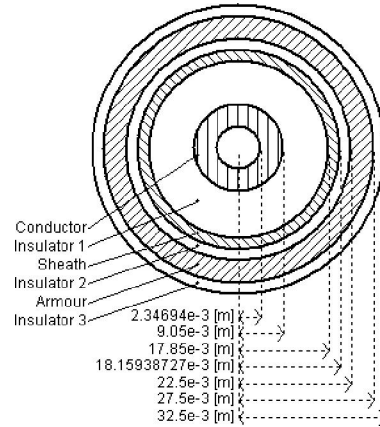

Fig. 2. The MV cables geometric configuration modeled in PSCAD/EMTDC.

Table 3: Wind Farm and Wind Turbine Transformers Data at 50 Hz.

Wind Turbine Transformers Model	
Connection method	Y / Δ
Voltage (line rms)	0.69 / 33.0 [kV]
Rated power	2.5 [MVA]
Leakage reactance	0.082573 [pu]
Copper losses	0.0084 [pu]
No-load losses	0.0022 [pu]
Wind Farm Transformer Model	
Connection method	Δ / Y / Δ
Voltage (line rms)	33.0 / 132.0 / 33.0 [kV]
Rated power	180.0 [MVA]
Leakage reactance	0.1 [pu]
Copper losses	0.004 [pu]
No-load losses	0.001 [pu]

D. Surge Arrester Modeling

In order to provide a protection for WTTs and MV submarine cables from switching overvoltage surges, it is assumed that surge arresters are installed at the MV side of each transformer as shown in Fig. 4.

The surge arresters are modeled as a nonlinear resistance with the V-I characteristics given in Table 4.   The burnout of an arrester occurs when the heat produced by the current flowing through the arrester exceeds its thermal limit [18].
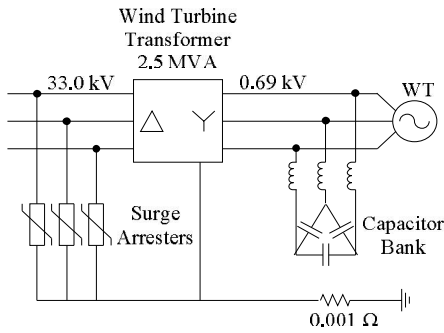
Fig. 3. Surge Arresters connected at wind turbine transformer.

Table 4: The V-I Characteristics of the Surge Arresters.

Voltage [kV]	Current [kA]
40.0	0.000001
50.0	0.001
55.265	0.01
65.79	0.1
74.5	1.0
86.85	3.1623
100.0	10.0
109.525	17.7828
111.4	21.54435
125.0	46.4159
150.0	100.0

E. **Capacitor Bank Modeling**

The capacitor bank is connected to the LV side of the WTT as shown in Fig. 3.   It is a common use in the capacitor banks to include a reactor before the capacitors in order to protect the banks. In this situation, the reactor is indirectly defined by the degree of inductance in the capacitor bank. This degree represents the ratio between the inductive and capacitive reactance of the equipment.   The reactance and capacitance in the capacitor bank can be calculated if the reactive power generation, the nominal frequency and the voltage on the LV side of the WTT are known [1].

4. Investigation of Ferroresonance Phenomenon in Offshore Wind Farm

In this section, ferroresonance phenomenon in offshore wind farm is investigated for three different abnormal switching operation**s.**

A. De-energization of Two Phases of the HV Side of WTT

In this subsection, the investigation of the ferroresonance phenomenon is implemented by the de-energization of both phases B and C of the HV side of WTT #A1. This abnormal switching

operation is implemented if the switch disconnecting fuses of phases B and C have blown. Also, the same abnormal switching operation is applied at phases B and C of the HV side of WTT#A9.

Fig. 4 shows the equivalent circuit of the WTT after fuses of phases B and C have blown out. C_{cable} represents the equivalent capacitance of the 33 kV submarine cables from the platform to the WTT HV side. $C_{H.G}$ and $C_{L.G}$ represent the stray capacitance from HV and LV sides to the ground, respectively. $C_{H.L}$ represents the stray capacitance from LV to HV side.   The typical values of the WTT stray capacitances are given by [19].

Although the WTT is not energized due to the opening of two phases, there is still a path for current through the two windings AB and AC of the delta connection and the single- core submarine cable capacitance of line A and also the WTT stray capacitances.   This current can produce ferroresonance and consequently impresses excessive overvoltages on the un-energized phases of the WTT.
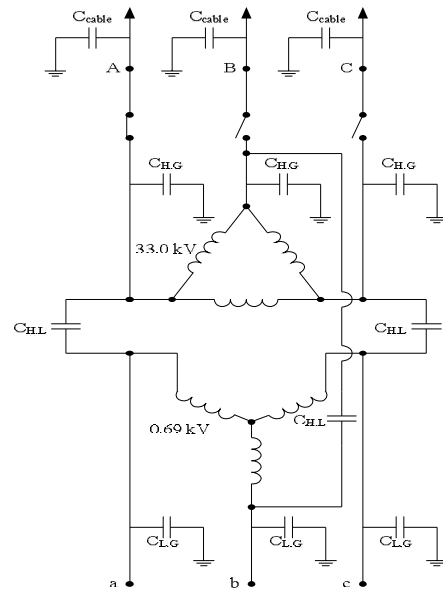

Fig. 4. Equivalent circuit of the WTT after the blow out of phases B and C fuses.

Fig. 5 shows the three-phases transient overvoltages on both HV side and LV side of WTT#A1 without surge arresters. It is clear that, the voltages of phases B and C at both HV side and LV side reach very high values beyond its nominal value so it causes excessive electrical stresses on the insulation of the WTT#A1.

Fig. 6 shows the three-phases transient overvoltages on both HV side and LV side of WTT#A1 with surge arresters. It is obvious that using surge arresters results in effective suppression

of ferroresonance phenomenon. The voltage of the de-energized phases, B and C, at both HV and LV sides is the same as voltage A after the suppression of ferroresonance as shown in Fig. 6.

Fig. 7 & 8 show the three-phases transient overvoltages on both HV side and LV side of WTT#A9 with and without surge arresters. From Fig. 7, it is shown that the voltages of the de-energized phases, B and C, exceeds their nominal value. With using surge arresters, the transient overvoltages and ferroresonance phenomenon are suppressed as shown in Fig. 8.

Although instant of the abnormal switching of both identical transformers WTT#A1 and WTT#A9 is the same, the transient overvoltages are different. This attributes to the change in the value of C_{cable} as shown in Fig. 4. Also, these transient overvoltages are different for both de-energized phases (*i.e.* phases B and C) at each WTT due to the change in point on voltage wave when the abnormal switching is performed.

Fig. 9 shows the absorbed energy in the three phase surge arresters at WTT #A1 and WTT #A9 (i.e. at both abnormal switching cases). It is clear that the absorbed energy in the surge arresters for both first and second switching operations is limited. This can be attributed to that the ferroresonance phenomenon of both first and second abnormal switching operations is suppressed by using the surge arresters only and not repeated.

B. De-energization of One Phase of the Single-Core Submarine Cable

In this subsection, the investigation of the ferroresonance phenomenon is implemented by de-energization of phase C of the single-core submarine cable. This abnormal switching operation is performed by opening the circuit breaker pole of phase C of row A. The transient overvoltage due to ferroresonance on both HV (33 kV) and LV (0.6kV) sides of WTTs are investigated. Also, the absorbed energy in the surge arresters which are connected to the HV terminals of WTTs of row A is investigated.

Fig. 10 shows the transient overvoltages on phase C of the single-core submarine cable of row A (*i.e.* on the HV side of all WTTs of row A) and on the LV side without surge arresters. It is clear that, the voltage on both HV and LV side reach very high values beyond its nominal value causing excessive electrical stresses on the insulation of both submarine cables and the WTTs of row A.
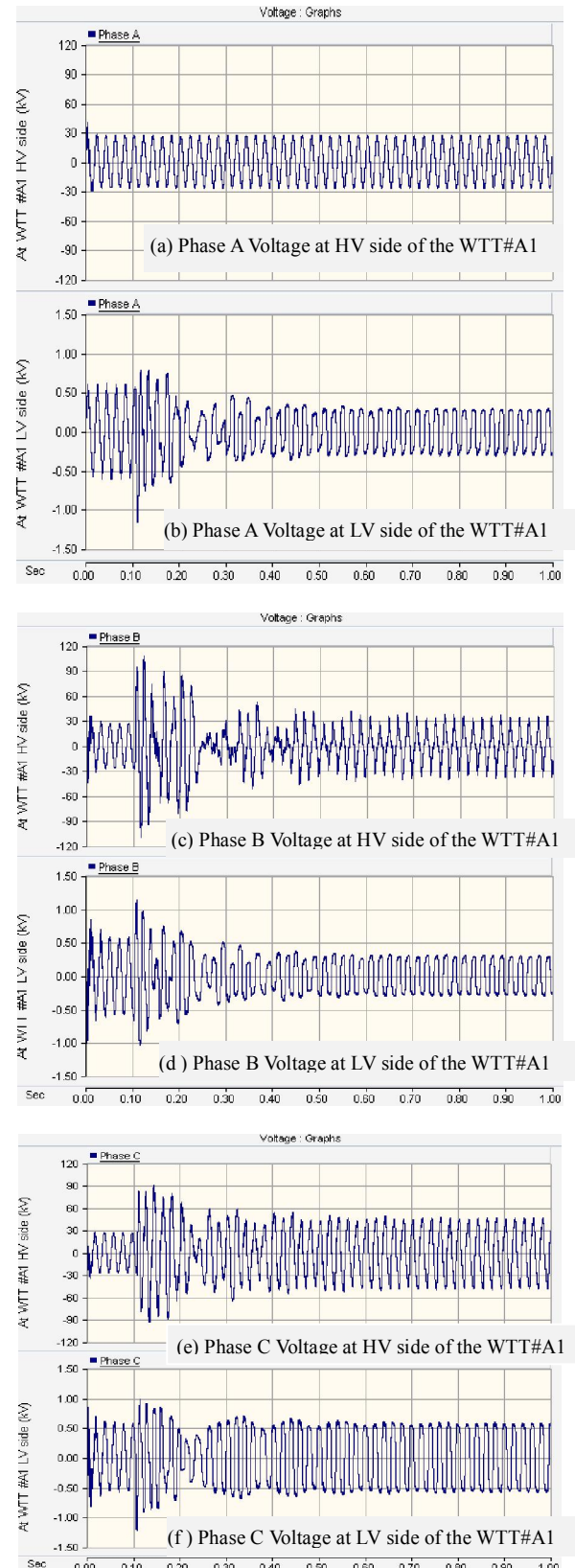

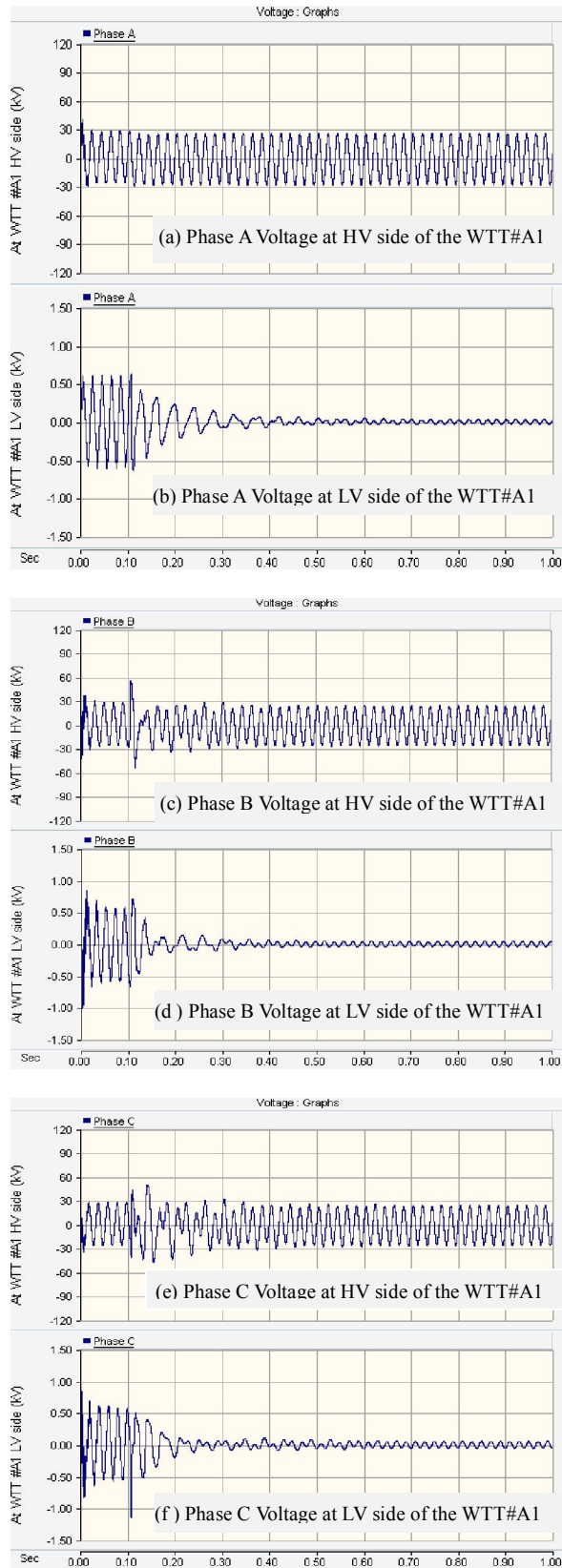Fig. 5. Transient overvoltage at both HV and LV sides of WTT#A1 without surge arresters.

945

(a) Phase A Voltage at HV side of the WTT#A1

(b) Phase A Voltage at LV side of the WTT#A1

(c) Phase B Voltage at HV side of the WTT#A1

(d) Phase B Voltage at LV side of the WTT#A1

(e) Phase C Voltage at HV side of the WTT#A1

(f) Phase C Voltage at LV side of the WTT#A1

Fig. 6. Transient overvoltage at both HV and LV
sides of WTT #A1 with surge arresters.

(a) Phase A Voltage at HV side of the WTT#A9

(b) Phase A Voltage at LV side of the WTT#A9

(c) Phase B Voltage at HV side of the WTT#A9

(d) Phase B Voltage at LV side of the WTT#A9

(e) Phase C Voltage at HV side of the WTT#A9

(f) Phase C Voltage at LV side of the WTT#A9
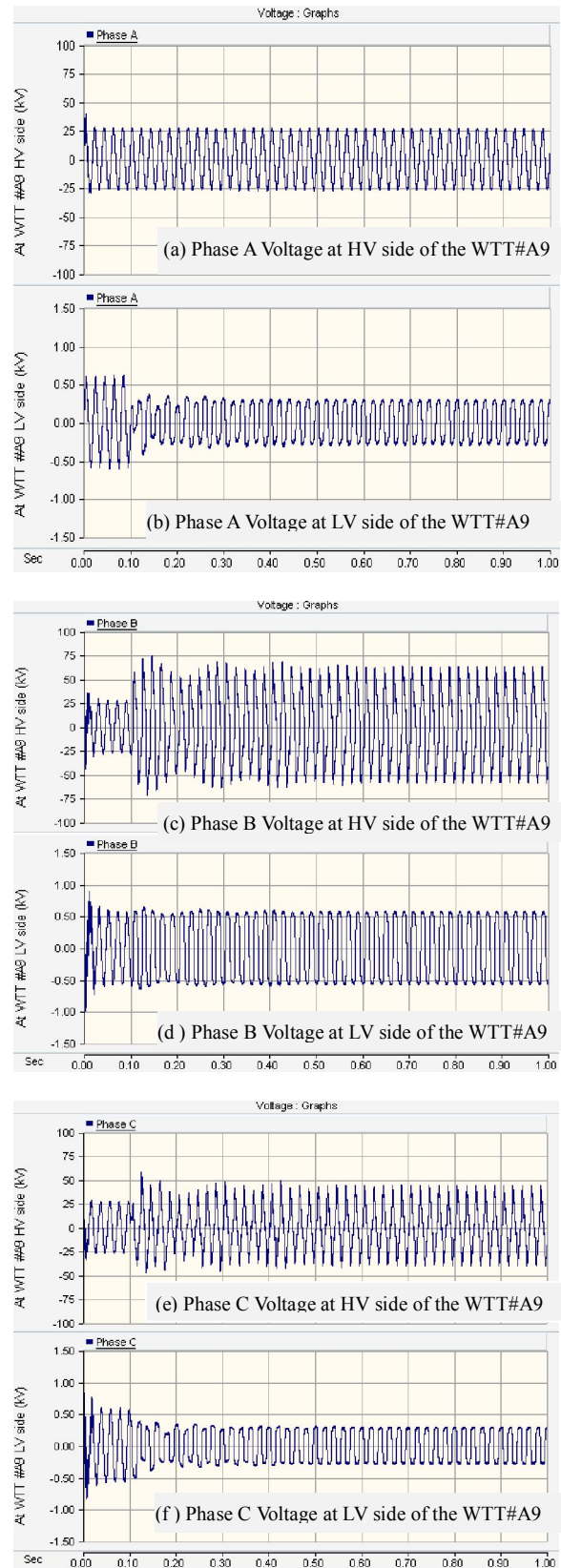
Fig. 7. Transient overvoltage at both HV and LV
sides of WTT #A9 without surge arresters.

(a) Phase A Voltage at HV side of the WTT#A9

(b) Phase A Voltage at LV side of the WTT#A9

(c) Phase B Voltage at HV side of the WTT#A9

(d) Phase B Voltage at LV side of the WTT#A9

(e) Phase C Voltage at HV side of the WTT#A9

(f) Phase C Voltage at LV side of the WTT#A9
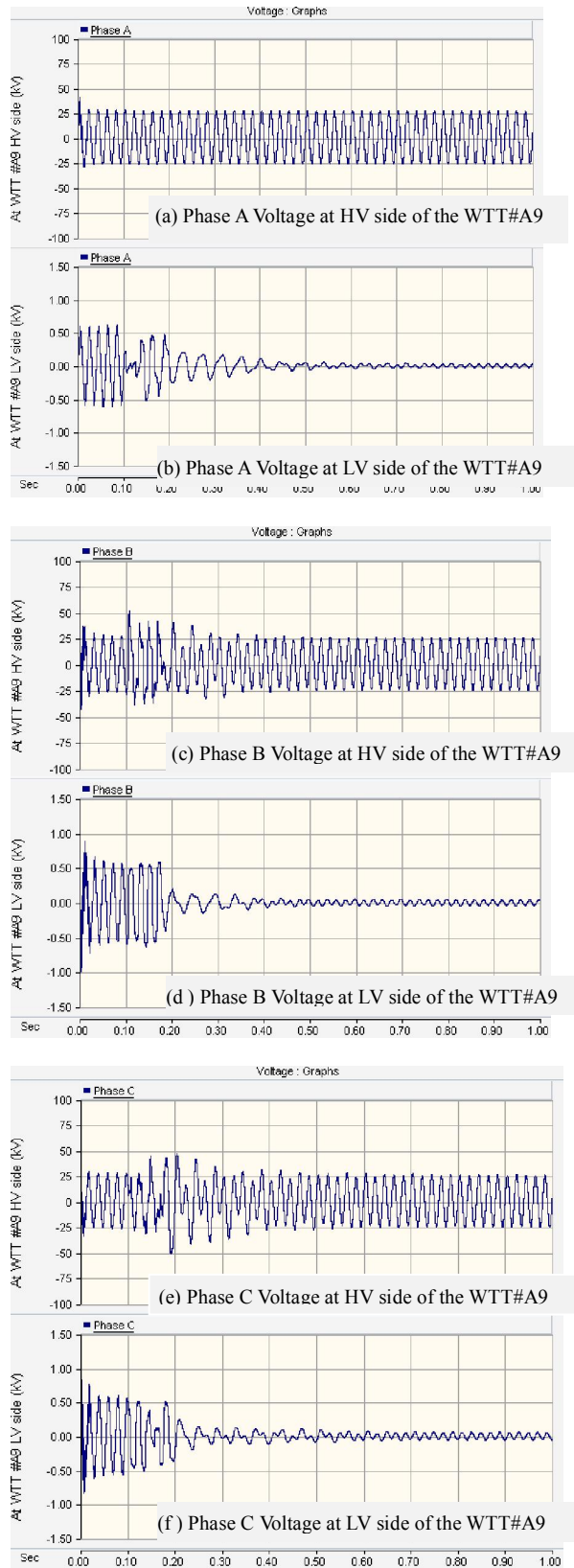
Fig. 8. Transient overvoltage at both HV and LV sides of WTT #A9 with surge arresters.

(a) Voltage at HV side

(a) At WTT#A1

Voltage at LV side

(b) At WTT#A9
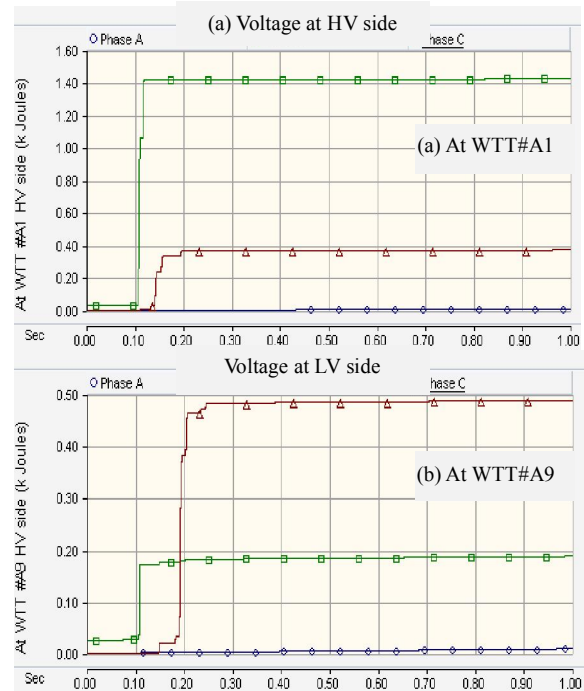
Fig. 9. The absorbed energy in the three-phase surge arresters for WTT #A1 and WTT #A9.

(a) Voltage at HV side

(b) Voltage at LV side
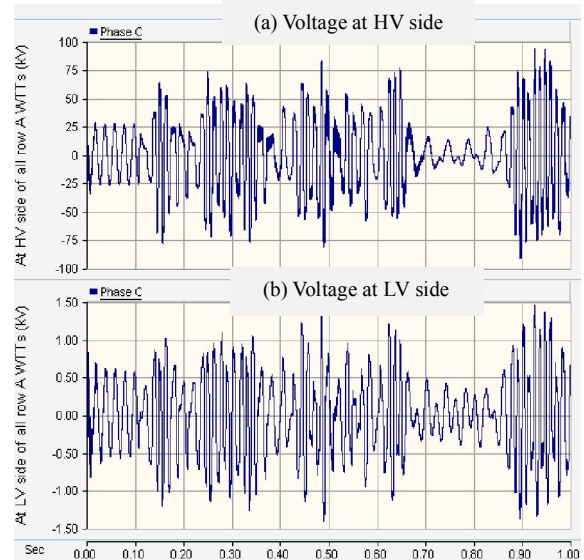
Fig. 10. Phase C overvoltage transients at both HV and LV sides of all WTTs in row A without surge arresters.

In order to suppress these excessive electrical stresses, surge arresters are connected to the HV side of all WTTs as shown in Figs. 3 & 11 shows the transient overvoltages on phase C of the single-core submarine cable of row A with surge arresters.   It is obvious that using surge arresters results in suppression of the transient overvoltages to a limited

value. From Fig. 11, it is clear that the ferroresonance phenomenon sustains which results in destroying and burning out the connected surge arresters. Therefore, the surge arresters are not sufficient for the suppression of ferroresonance phenomenon of the first abnormal switching operation. Therefore, the absorbed energy in surge arrester of phase C at all WTTs of row A increases continuously as shown in Fig. 12 due to the repeated ferroresonance. Consequently, the surge arresters are destroyed and burnt out as soon as the generated heat in the surge arresters exceeds the thermal limit.
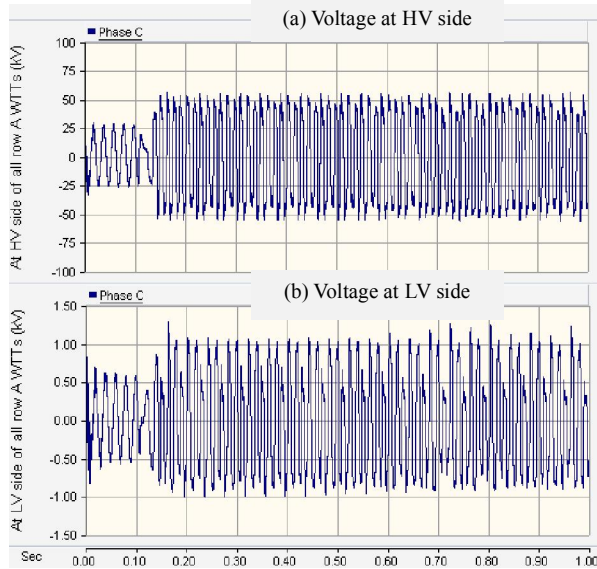

Fig. 11. Phase C transient overvoltage at both HV and LV sides of all WTTs in row A with surge arresters.

5. The Proposed Protective Method for the Suppression of Repeated Ferroresonance Phenomenon

In this section, a protective method is proposed for the suppression of repeated ferroresonance phenomenon which appears in the first abnormal switching operation as illustrated in the previous section. Consequently, this proposed protective method results in preventing the surge arresters from damage and burning out which happen due to the continuous overvoltages caused by the repeated ferroresonance.

Fig. 13 shows this proposed protective method which consists of three-phase star connected resistors of 12.0 Ω for each one. These resistors are connected on the LV side of the WTT through three-phase controlled switch. If the heat generated in the surge arresters exceeds a certain limit, E_0, the controlled switch operates and connects these resistors for 0.5 second.
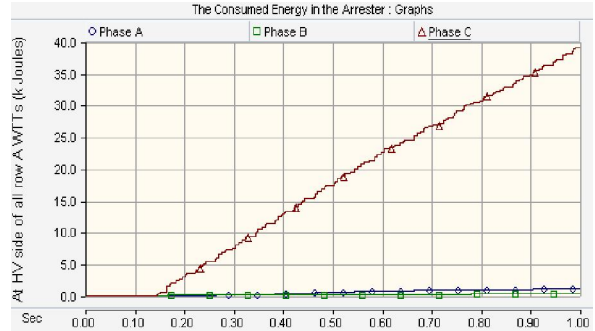

Fig. 12. The absorbed energy in the three-phase surge arresters for each WTT in row A.
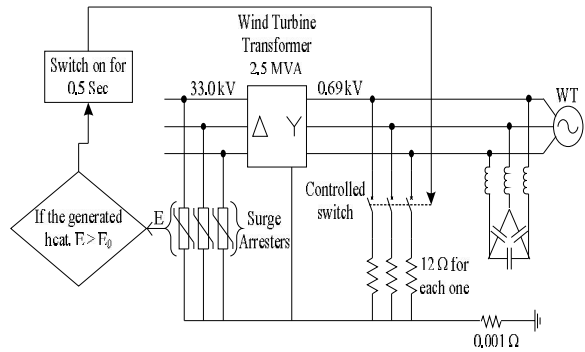

Fig. 13. The proposed protective method for the suppression of repeated ferroresonance phenomenon in first abnormal switching operation.
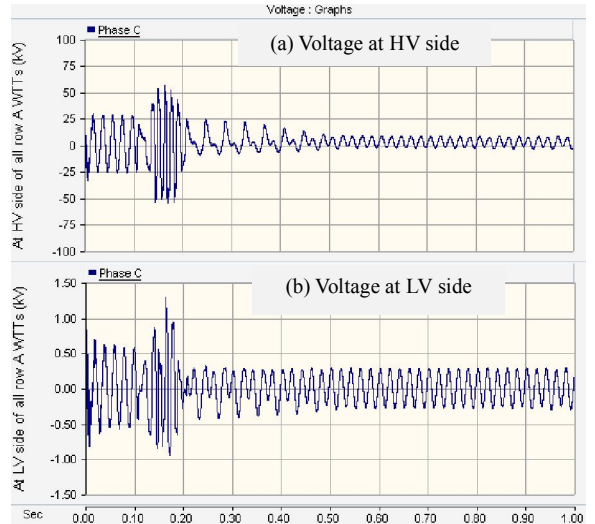

Fig. 14. Phase C transient overvoltage at both HV and LV sides of all WTTs in row A with surge arresters and the proposed protective method.

Fig. 14 shows the transient overvoltages on phase C of the single-core submarine cable of row A with surge arresters when the proposed protective method is applied. From Fig. 14, it is obvious that using this protective method results in suppression of the

repeated ferroresonance phenomenon as the transient overvoltages of the de-energized phase (*i.e.* phase C) are eliminated. The controlled switch operates at 0.1759 second. It is clear that after the opening of the controlled switch at 0.6759 second, ferroresonance phenomenon vanishes. Therefore, this method is an effective method for the protection of surge arresters against the continuous transient overvoltages due to the repeated ferroresonance phenomenon in the offshore wind farms.

Therefore, the absorbed energy in the surge arrester of phase C at all WTTs of row A is limited at a certain value as shown in Fig. 15 and consequently the surge arresters are protected from damage and burning out.
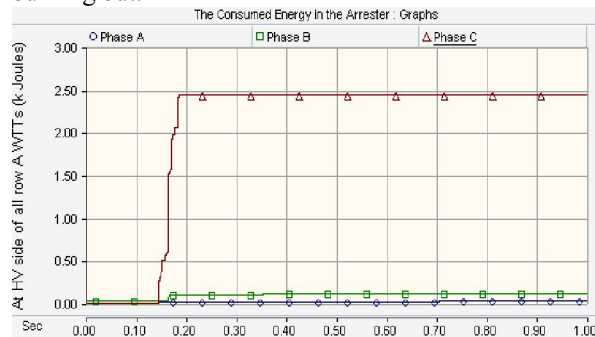

Fig. 15. The absorbed energy in the three-phase surge arresters for each WTT in row A with applying the proposed protective method.

Conclusion

This paper investigates the ferroresonance phenomenon due to abnormal switching operations in offshore wind farms.

The abnormal switching operations of de-energization of two phases on the HV side of the first and last WTTs of one row are applied. These switching operations are performed by the blow out of the switch disconnecting fuses. The results show that there are transient overvoltage on both de-energized phases. The transient overvoltages are different for both cases due to the change in the cable capacitance due to the change in cable length from the platform to the investigated WTT. Also, these transient overvoltages are different for both de-energized phases at each WTT due to the change in point on voltage wave when the abnormal switching is performed. Surge arresters are used for the suppression of these transient overvoltages. The results show also that the surge arresters suppress the ferroresonance and the absorbed energy in the surge arresters are limited under their thermal limit.

Furthermore, de-energization of one phase of a three-phase single-core submarine cable of one row in the offshore wind farm is applied. This switching operations are performed by the opening of one pole of the three-phase circuit breaker at the platform. The results show high transient overvoltages on the de-energized phases which causes severe electrical stresses on the insulations. Although surge arresters are used, the sustaining ferroresonance overvoltage may cause damage for the surge arresters.

A protective method for suppression the ferroresonance is proposed. The results show that the proposed protective method gives high suppression to ferroresonance in offshore wind farms and the surge arresters are protected against burning out.

Corresponding author
Ebrahim A. Badran
Electrical Engineering Department, Faculty of Engineering, Mansoura University, Mansoura, Egypt
ebadran@mans.edu.eg

References

[1] Iván Arana Aristi (2008). Modeling of Switching Transients in Nysted Offshore Wind Farm and a Comparison with Measurements," Master of Science Thesis, June 2008, Technical University of Denmark.

[2] Arana I., J. Holbøll, T. Sørensen, A. H. Nielsen, P. Sørensen, O. Holmstrøm (2009). Comparison of Measured Transient Overvoltages in the Collection Grid of Nysted Offshore Wind Farm with EMT Simulations," International Conference on Power Systems Transients (IPST2009) in Kyoto, Japan June 3-6, 2009.

[3] Poul Sørensen, Anca D. Hansen, Troels Sørensen, Christian S. Nielsen, Henny K. Nielsen, Leif Christensen, Morten Ulletved (2007). Switching transients in wind farm grids. available at www.ewec2007proceedings.info/allfiles2/418_Ewec2007fullpaper.pdf

[4] Lars Liljestrand, Ambra Sannino*, Henrik Breder and Stefan Thorburn (2008). Transients in Collection Grids of Large Offshore Wind Parks. Wind Energy. 2008; 11:45–61 Published online 2 July 2007 in Wiley Interscience.

[5] Greenwood A. (1991). Electrical Transients in Power Systems", 2nd Edition, Wiley Interscience.

[6] Zia Emin, Yu Kwong Tong (2001). Ferroresonance Experience in UK: Simulations and Measurements," International Conference on Power Systems Transients (IPST2001) in Rio de Janeiro, Brazil on June 24-28, 2001, paper no.6.

[7] Preecha Sakarung, Somchai Chatratana (2005). Application of PSCAD/EMTDC and Chaos Theory to Power System Ferroresonance

Analysis. International Conference on Power Systems Transients (IPST'05) in Montreal, Canada on June 19-23, 2005Paper No. IPST05 – 227

[8] Roger C. Dugan (2009).Examples of Ferroresonance in Distribution Systems," available at www.ece.mtu.edu/faculty/bamork.

[9] Pattanapakdee K. and C. Banmongkol (2007). "Failure of Riser Pole Arrester due to Station Service Transformer Ferroresonance," International Conference on Power Systems Transients (IPST'07) in Lyon, France on June 4-7.

[10] Surya Santoso, Roger C. Dugan, Thomas E. Grebe, Peter Nedwick (2001). Modeling Ferroresonance Phenomena in an Underground Distribution System," International Conference on Power Systems Transients (IPST2001) in Rio de Janeiro, Brazil on June 24-28, 2001, paper no.34.

[11] Technical documentation, "ABB XLPE Cables User's Guide," which is available at www.abb.com.

[12] Martinez J. A., B. Gustavsen, and D. Durbak (2005). Parameter Determination for Modeling System Transients Part II: Insulated Cables," IEEE Transactions on Power Delivery, 20(3): 2045-2050.

[13] Abey Daniel and Samson Gebre (2008). Analysis of Transients in Wind Parks: Modeling of System Components and Experimental Verification," MSc in Electric Power Engineering, Chalmers University of Technology, Göteborg, Sweden.

[14] Daniel Mireanu (2007). Transient Over-voltages in Cable Systems - Part 1 – Theoretical analysis of large cable systems. Master of Science Thesis, Chalmers University of Technology, Göteborg, Sweden.

[15] Maialen Boyra (2007).Transient Over-voltages in Cable Systems - Part 2 – Experiments on fast transients in cable systems. Master of Science Thesis, Chalmers University of Technology, Göteborg, Sweden.

[16] "PSCAD/EMTDC USER'S GUIDE," Copyright 2005 Manitoba HVDC Research Centre.

[17] Mukesh Nagpal, Terrence G. Martinich, Ali Moshref, Kip Morison, and P. Kundur (2006). Assessing and Limiting Impact of Transformer Inrush Current on Power Quality," IEEE Transactions on Power Delivery, 21(2): 890-896.

[18] Yoh Yasuda, Hayato Kobayashi and Toshihisa Funabashi (2008). Surge Analysis on Wind Farm When Winter Lightning Strikes. IEEE Transactions on Energy Conversion, 23(1): 257-262.

[19] Tarik Abdulahovic (2009). Analysis of High Frequency Electrical Transients in Offshore Wind Parks," Thesis for the degree of licentitate of engineering, Chalmers University of Technology, Göteborg, Sweden.

8/21/2011